Leukemia
https://doi.org/10.1038/s41375-018-0355-y

ARTICLE

Lymphoma

Functional cooperativity of p97 and histone deacetylase 6 in mediating DNA repair in mantle cell lymphoma cells

Pratikkumar H. Vekaria[1] · Amar Kumar[1] · Dharmalingam Subramaniam[2] · Neil Dunavin[1] · Anusha Vallurupalli[1] · Frank Schoenen[3] · Siddhartha Ganguly[1] · Shrikant Anant[2] · Joseph P. McGuirk[1] · Roy A. Jensen[4] · Rekha Rao[1,2]

Received: 18 June 2018 / Revised: 15 October 2018 / Accepted: 12 November 2018

Abstract

p97 is an ATPase that works in concert with histone deacetylase 6 (HDAC6), to facilitate the degradation of misfolded proteins by autophagosomes. p97 has also been implicated in DNA repair and maintaining genomic stability. In this study, we determined the effect of combined inhibition of p97 and HDAC6 activities in mantle cell lymphoma (MCL) cells. We report that treatment with p97 inhibitors induces dose-dependent apoptosis in MCL cells. The p97 inhibitor CB-5083 induces ER stress markers GRP78 and CHOP and results in the accumulation of polyubiquitylated proteins. Co-treatment with CB-5083 and the HDAC6 inhibitor ACY-1215 result in marked downregulation of CDK4, Cyclin D1, and BRCA1 levels without inhibiting autophagic flux. Consequently, treatment with CB-5083 accentuates DNA damage in response to treatment with ACY-1215 resulting in enhanced accumulation of H2AX-γ and synergistic apoptosis. Furthermore, ATM loss severely impairs phosphorylation of 53BP1 following co-treatment with CB-5083 and ACY-1215 in response to gamma irradiation. Finally, co-treatment CB-5083 and ACY-1215 results in reduced tumor volumes and improves survival in Z138C and Jeko-1 xenografts in NSG mice. These observations suggest that combined inhibition of p97 and HDAC6 abrogates resolution of proteotoxic stress and impairs DNA repair mechanisms in MCL cells.

Introduction

Mantle cell lymphoma (MCL) is a rare but aggressive subtype of non-Hodgkin's lymphoma which is characterized by constitutive expression of cyclin D1 (*CCND1*) [1]. Other recurrent genetic mutations in MCL include mutations in *ATM, p53*, and *CCND1*, as well as the activation of signaling pathways including that of B-cell receptor (BCR), phosphoinositide-3 kinase (PI3K), and nuclear factor-kappa B (NF-κB) [2, 3].

MCL cells are sensitive to agents (such as bortezomib, pan-HDAC inhibitors, or their combination) that disrupt protein homeostasis and induce proteotoxic stress [4]. We therefore reasoned that p97, or valosin-containing protein (*VCP*), could be a potential therapeutic target in MCL, owing to its ability to resolve proteotoxic stress. p97 is a segregase with ATPase activity that works in concert with the ubiquitin proteasome system to remodel protein complexes and restore protein homeostasis [5, 6]. In a process called endoplasmic reticulum-associated degradation (ERAD), p97 promotes the retrotranslocation of misfolded, ubiquitylated proteins from the ER and facilitates their proteasomal degradation [7]. p97 inhibition has emerged as a novel therapeutic target in cancer cells—especially those that depend on high protein turnover and/or ER function [8, 9].

p97 serves as a modulator of genome stability by participating in DNA replication, transcription, and repair mechanisms. Double-stranded DNA breaks (DSBs) induce the ubiquitin ligase RNF8 and RNF168-mediated

Supplementary information The online version of this article (https://doi.org/10.1038/s41375-018-0355-y) contains supplementary material, which is available to authorized users.

✉ Rekha Rao
rraomanepalli@kumc.edu

[1] Division of Hematologic Malignancies and Cellular Therapeutics, The University of Kansas Cancer Center, Kanas City, KS, USA

[2] Department of Cancer Biology, The University of Kansas Cancer Center, Kanas City, KS, USA

[3] Higuchi Biosciences Center, University of Kansas, Lawrence, KS, USA

[4] Department of Pathology & Laboratory Medicine, The University of Kansas Cancer Center, Kansas City, KS, USA

Published online: 21 January 2019

ubiquitylation of the histone H2A (H2AK15). In association with its cofactor Ufd1-Npl4, p97 recognizes ubiquitylated H2AK15 and facilitates the recruitment of additional DNA repair proteins, such as Ku80 and the H4K20me2-binding protein 53BP1 onto DSBs, which participate in non-homologous end joining (NHEJ) DNA repair [10, 11]. This process is regulated by DNA-damage-induced phosphorylation of 53BP1 by ataxia-telangiectasia mutated (ATM) and ATR (ATM and Rad3 Related) protein kinases throughout the interphase [10, 11]. In contrast to NHEJ pathway, cells in the G2 and S phases of the cell cycle repair DNA by homologous recombination (HR) pathway in a process that involves DNA end resection. p97-mediated release of Ku proteins and 53BP1 from DSBs commits the cells to HR and promotes the recruitment of HR-associated repair proteins, such as Rad51 and BRCA1 on DSBs [12, 13].

p97-dependent homeostatic pathways intersect with histone deacetylase 6 (HDAC6) protein in the clearance of ubiquitylated misfolded proteins. In complex with p97 and HSP90, HDAC6 regulates reversible deacetylation of the molecular chaperone HSP90 [14, 15]. Hyperacetylation of HSP90 in response to treatment with pan-HDAC inhibitors or HSP90 inhibitors, impairs maturation of a myriad of HSP90 "client proteins" including BRCA1, CDK4 as well as HDAC6 [16–18]. Under conditions that induce proteotoxic stress, p97 facilitates the extraction of HDAC6 from polyubiquitylated proteins to restore the formation of the HSP90-HDAC6 complex [14]. Furthermore, by binding to and shuttling misfolded, ubiquitylated proteins through its c-terminus Zinc finger domain, HDAC6 facilitates their sequestration into cytoprotective aggresomes which are degraded by the fusion of autophagosomes with lysosomes [19, 20].

It is presently unclear whether disrupting the functional cooperativity between HDAC6 and p97 affects MCL-cell survival. In this study, we report the synergistic activity of p97 inhibitors with the HDAC6-selective inhibitor, ACY-1215 in MCL cells. Our studies further explore the intersection of p97 and HDAC6 functions in autophagy and DNA repair in MCL cells [21].

Materials and methods

Cell culture, p97 inhibitors, and antibodies

Human MCL cell lines MO2058, JeKo-1, and Z138C were cultured as described previously [4]. Rec-1 and JVM-2 cells were obtained from ATCC. All cells were screened for cyclin D1 expression and authenticated from University of Arizona Genetics Core every 6 months. All primary de-linked de-identified MCL samples were procured after informed consent through an institutionally approved protocol (HSC-5929). B cells were isolated from MCL specimens as described previously [22]. p97 inhibitors DBeQ and NMS-873 were obtained from Selleck chemicals (Houston, TX), ML240 was obtained from Sigma Aldrich (St. Louis, MO) and ACY-1215 and CB-5083 were obtained from MedChem Express (NJ)

Western blot analyses

Western blot analyses were performed using specific antisera or monoclonal antibodies as described previously [4]. Blots were scanned and quantified with Odessey Infrared Scanning System. List of antibodies and their source is available in supplementary Figure 1S. All western blots data were repeated three independent times.

Proteostat staining and confocal immunofluorescent microscopy

MCL cells were stained with LC3B-II antibodies as described previously [4]. Proteostat staining was performed as per manufacturer's instructions (Enzo LifeSciences, NY) [23]. The slides were imaged using Carl Zeiss Pascal confocal microscope at ×63 magnification. The experiments were repeated three independent times.

Annexin V-propidium iodide staining and cell cycle analysis

MCL cell lines were exposed to indicated-concentrations of drugs for 24–48 h and apoptotic cells were assessed using a BD Accuri flow cytometer [4]. All experiments were repeated three times to obtain standard deviation of the mean values. Synergistic interactions for the combination of drugs were assessed using the median dose effect of Chou–Talalay. Combination index (CI) for each drug was obtained using the commercially available software Calcusyn (Biosoft, Ferguson, MO) [4]. Alternatively, cell cycle analysis was performed as described previously [4].

Transfection and lentiviral knockdown of HDAC6

Z138C cells were transiently transfected by nucleofection using non-targeted (NT) RNA or siRNA smartpool for p97 (Dharmacon) utilizing the Human B cell transfection kit (program U-015). Jeko-1 cells were transfected with siRNA utilizing Xtremegene siRNA transfection kit (Sigma Aldrich, St. Louis). HDAC6 was knocked down with lentiviral Mission shRNA (Sigma Aldrich, St. Louis) in Jeko-1 and Z138C cells.

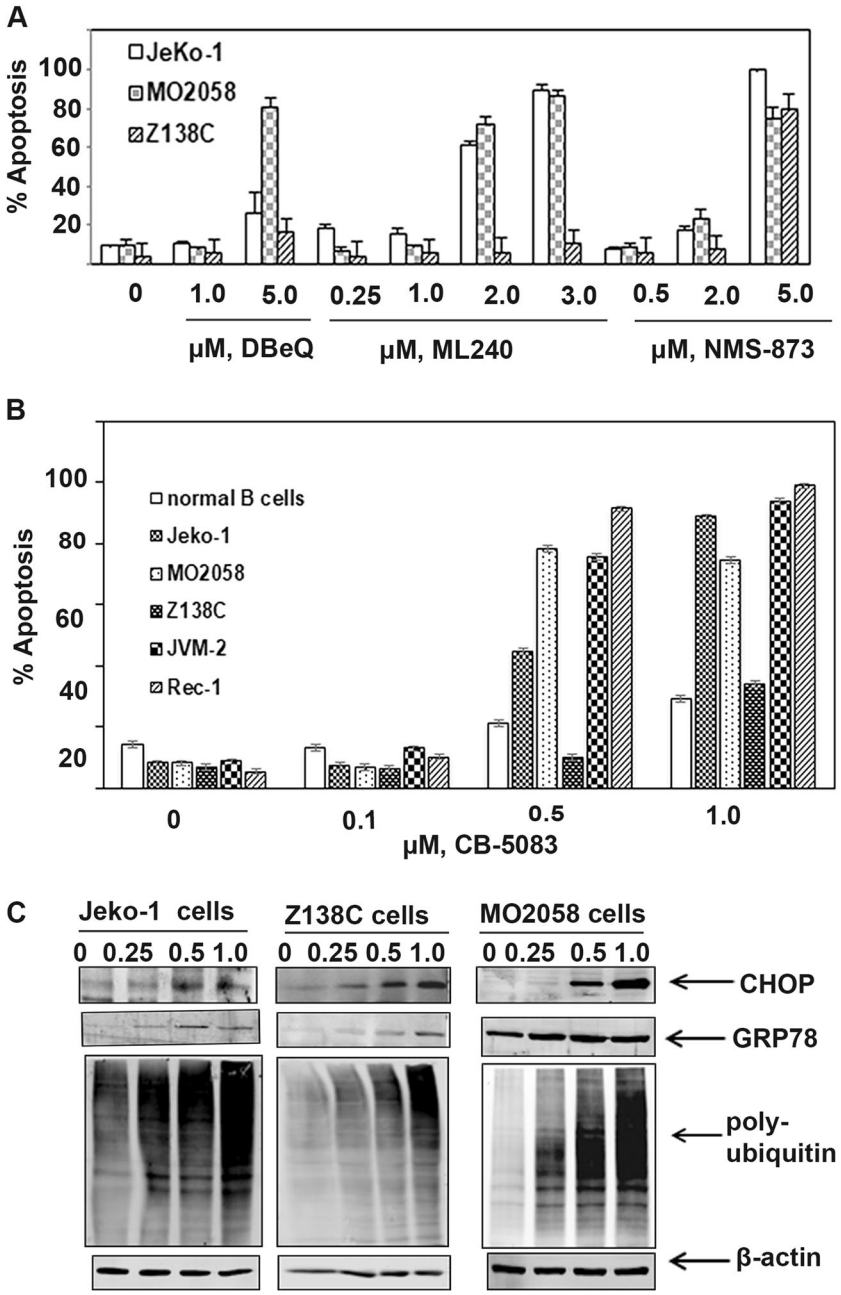

Fig. 1 Treatment with p97 inhibitors induces apoptosis in MCL cells. **a**, **b** Jeko-1, MO2058, and Z138C cells were treated with increasing concentrations of DBeQ, ML240, NMS-873, and CB-5083 for 48 h. The percentage of cells undergoing apoptosis was determined by Annexin-V-FITC and propidium iodide staining followed by flow cytometry. **c** MCL cell lines were treated with the indicated doses of CB-5083 for 6 h and the levels of polyubiquitylated proteins, CHOP, and GRP78 were determined by immunoblot analysis

In vivo studies with MCL cells xenograft

In vivo studies were carried out in accordance with an institutional animal care and use committee-approved protocol (2016-2352). MCL xenografts were generated by injecting 2.5 million Z138C cells or 3 million Jeko-1 into the flanks of NOD-SCID-*IL2rg*-/- (NSG) mice ($N = 6$ per group). Mice were randomized based on tumor volumes (average = 200 mm^3). Mice were administered with vehicle (hydroxyl propyl methyl cellulose), CB-5083 (40 mg/kg p.o., on a 4 days on and 3 days off schedule), ACY-1215 (40 mg/kg intraperitoneally, on a 5 days on and 2 days off schedule) or the combination of CB-5083 and ACY1215. All treatments were unblinded. Treatment was continued for 2 weeks and mice were humanely sacrificed when the tumor volume reached 2000 mm^3. Survival was plotted on a Kaplan–Meier plot as described previously [4]. Kaplan–Meier survival curves were performed with Log Rank test. All the tests were two-sided with significance level of 0.05.

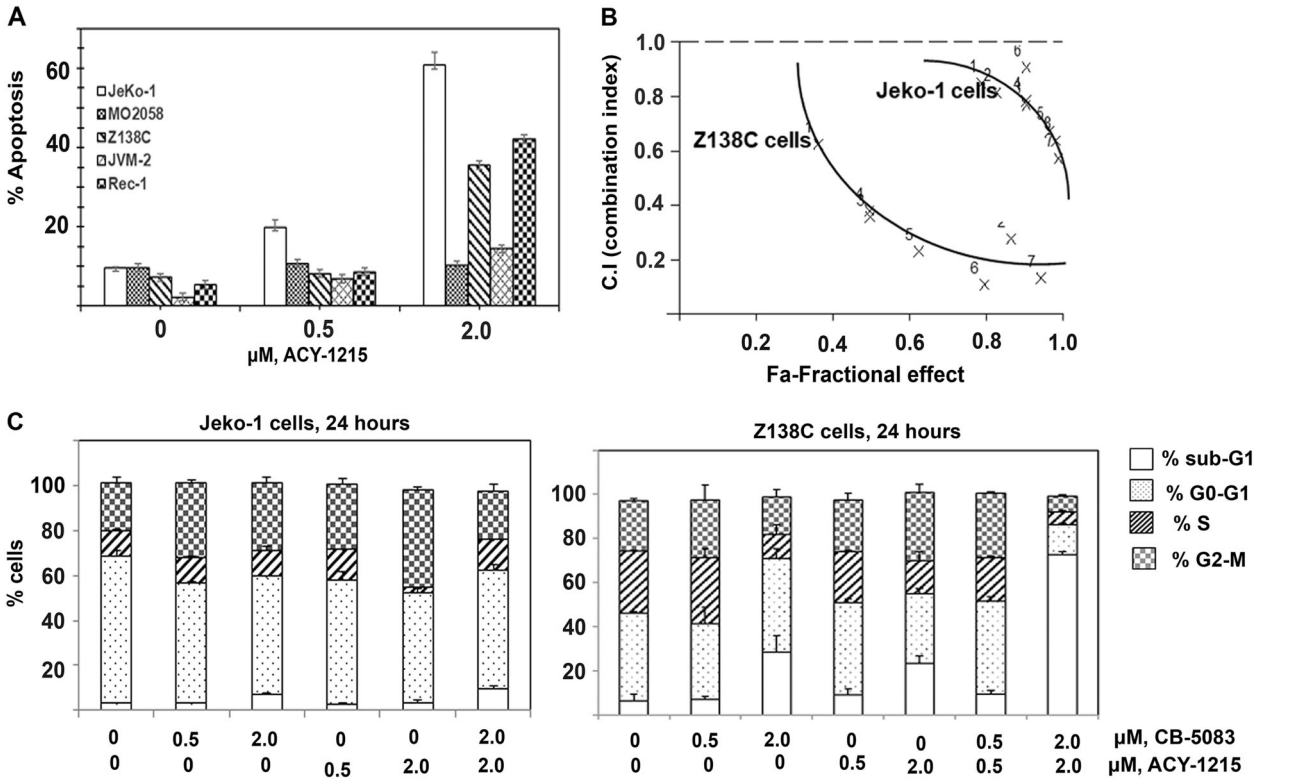

Fig. 2 Co-treatment with CB-5083 and ACY-1215 induces synergistic apoptosis in MCL cells. **a** Jeko-1, MO2058, and Z138C MCL cell lines were exposed to ACY-1215 for 48 h or in **b** exposed to the indicated doses of CB-5083 and ACY-1215 for 24 h. The percentage of apoptotic cells was determined by flow cytometry. CI values of <1.0 represent synergistic interaction of the two drugs

Results

Sensitivity of MCL cells to p97 inhibitors in vitro

In order to determine the effect of p97 inhibition on MCL cells, we exposed cultured MCL cell lines to a series of p97 inhibitors, such as DBeQ, ML-240, NMS-873, and CB-5083 [24–27]. Our studies demonstrate that most MCL cell lines tested are sensitive to p97 inhibitors, with Z138C being the least sensitive (Fig. 1a, b). We next determined the effect of p97 on the induction of ER stress in MCL cells. We observed that p97 inhibition with CB-5083-induced CHOP (an ER-stress inducible pro-apoptotic transcription factor) and GRP78 (an ER-resident HSP70 homolog) in MCL cells (Fig. 1c) [28]. Consistent with the reported effects of p97 inhibition on cellular protein homeostasis, treatment with CB-5083 resulted in the accumulation of polyubiquitylated proteins in MCL cells lines.

Co-treatment with p97 inhibitors with HDAC6 inhibitors induces synergistic apoptosis in MCL cells

In order to define novel therapeutic strategies that could potentially improve the anti-MCL activity of p97 inhibitors, we tested the effect of the combination of the HDAC6 selective inhibitor ACY-1215 with CB-5083 treatment in MCL cells. We reasoned that inhibiting p97 function, as well as HDAC6 activity would lead to the accumulation of ubiquitylated protein aggregates leading to proteotoxicity-induced cell death [4, 15]. We observed that while ACY-1215 induces modest apoptosis at low-micromolar concentrations in MCL cell lines, co-treatment with p97 inhibitors ML240 and CB-5083 with ACY-1215 induces synergistic apoptosis in cultured MCL cells (Fig. 2a, b and Supplementary Figure 2S). We observed that treatment with either CB-5083 or ACY-1215 alone results in accumulation of cells in G2-M phase in both Jeko-1 and Z138C cells and 80% of cells in sub-G1 phase in Z138C cells (Fig. 2c).

We next determined whether the combination of CB-5083 and ACY-1215 induces more ER stress than treatment with either agent alone in MCL cells. As expected, treatment with ACY-1215 induces the acetylation of tubulin (a bona fide substrate of HDAC6) in Jeko-1, Z138C, and Rec-1 cells [29] (Fig. 3a), without affecting the levels of p97 at 6 h. Co-treatment with CB-5083 and ACY-125 induces the expression of GRP78 and CHOP (Fig. 3b) with a modest increase in polyubiquitylated proteins in MCL cells (Fig. 3b).

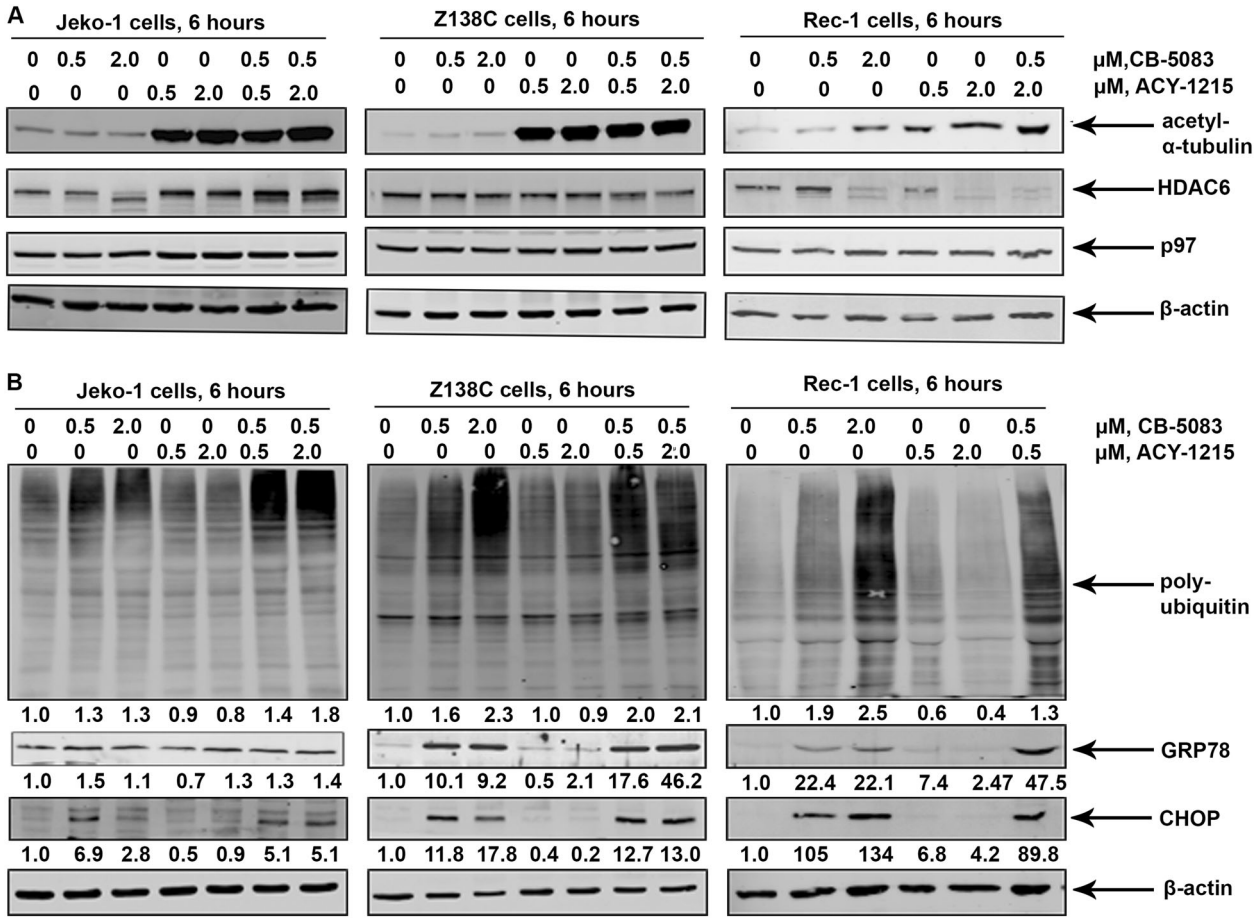

Fig. 3 Treatment with CB-5083 and ACY-1215 induces of ER stress and alters cell cycle distribution in MCL cells. **a**, **b** Jeko-1 and Z138C cells were exposed to the indicated concentrations of CB-5083 and ACY-1215 for 6 h and the expression of the indicated ER stress markers and polyubiquitylated proteins was determined by immunoblot analysis. **c** Jeko-1 and Z138C cells were exposed to indicated concentrations of CB-5083 and ACY-1215 for 24 h and the cell cycle distribution was determined by flow cytometry

Effect of co-treatment with CB-5083 and ACY-1215 on the autophagic clearance of misfolded proteins in MCL cells

A demonstrated effect of p97 inhibition and induction of ER stress is the activation of autophagy [30]. Unlike the documented effect of p97 inhibitors on the induction of LC3B lipidation (LC3B-II), CB-5083 does not result in the increase in LC3B-II in Jeko-1 and Z138C cells (Fig. 4a) [24, 25, 31]. Treatment with chloroquine (a lysosome inhibitor) induces LC3B-II suggesting that autophagy initiation is not inhibited in both cell lines (Fig. 4a).

We then determined whether CB-5083 and ACY-1215 altered the levels of p62 (an autophagic substrate which is degraded upon completion of autophagy) [31]. Interestingly, both Jeko-1 and Z138C cells show a decrease in the levels of p62 following treatment with CB-5083 and the co-treatment with CB-5083 and ACY-1215 (Fig. 4a). The potential implications of these observations are discussed below (see Discussion). Finally, we determined the effect of treatment with CB-5083 and ACY-1215 on the accumulation of misfolded proteins in MCL cells. We observed that both CB-5083 and ACY-1215 treatments result in enhanced fluorescence of Proteostat dye (a marker of enhanced aggregated protein inclusions) and co-localization of LC3-B puncta in Jeko-1 compared to control cells. Although Z138C also show enhanced Proteostat staining, it does not exhibit punctate LC3-B staining.

siRNA-mediated knockdown of p97 potentiates ACY-1215 induced DNA damage in MCL Cells

Given that CHOP is an ER-stress-induced transcription factor that is also upregulated in response to DNA damage, we tested the effect of p97 knockdown on the induction of DNA damage in MCL cells [32, 33]. siRNA-mediated partial knockdown of p97 does not induce the phosphorylation of H2AX (Fig. 5a). However, treatment with ACY-1215 accentuates the extent of H2AX phosphorylation following knockdown of p97 compared to NT siRNA

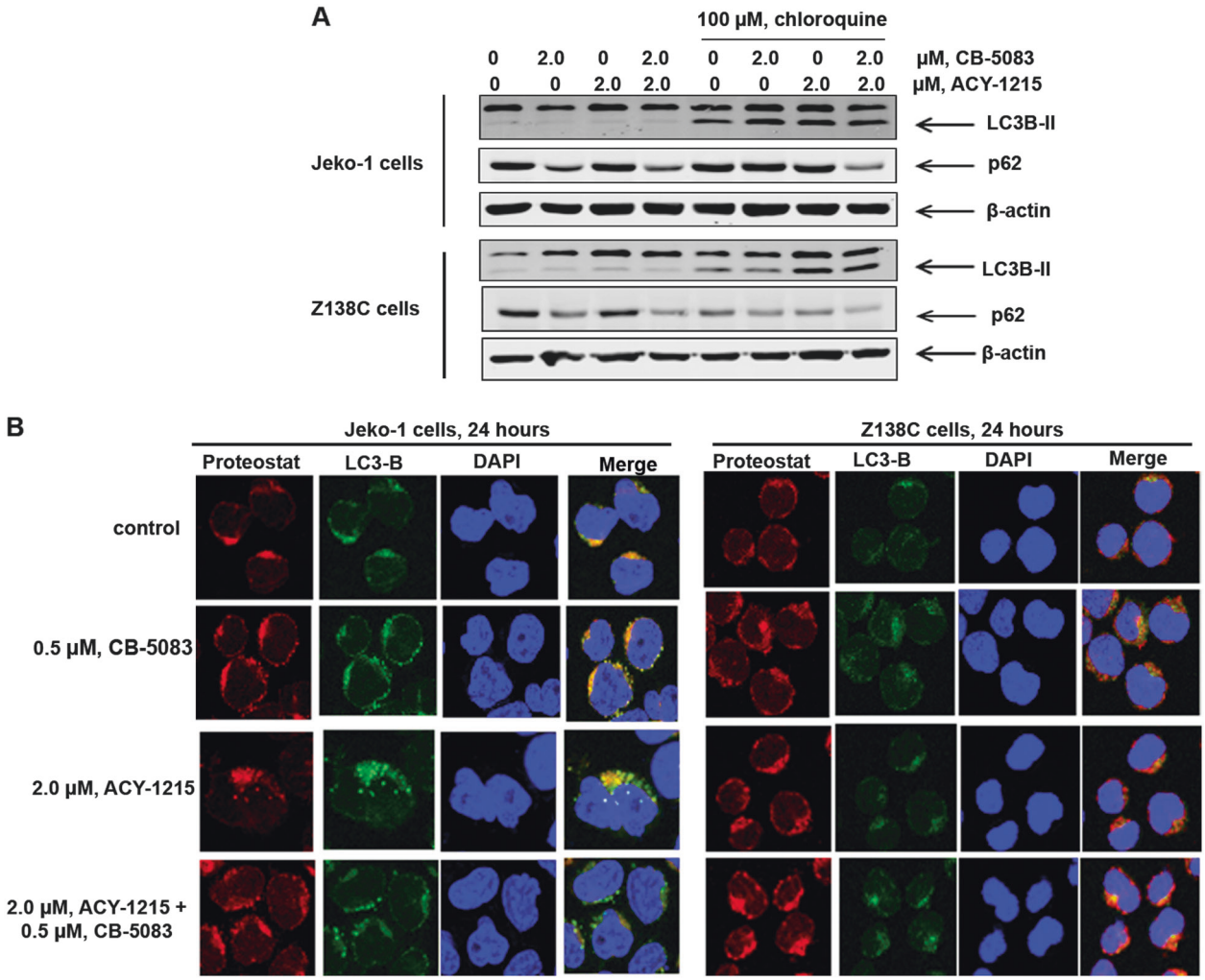

Fig. 4 Effect of co-treatment with CB-5083 and ACY-1215 on autophagy and accumulation of misfolded proteins. **a** Jeko-1 and Z138C cells were exposed to the indicated concentrations of CB-5083 and ACY-1215 in the presence or absence of the autophagy inhibitor chloroquine for 6 h and LC3B-II and p62 expression was assessed by immunoblot analysis. **b** Jeko-1 and Z138C cells were exposed to CB-5083 and ACY-1215 for 6 h and the cells were stained with proteostat stain (red) for an additional 30 min. The cells were then immunostained for LC3B (green) and counterstained with DAPI

controls. This is accompanied by enhanced expression of cleaved caspase 3 and down regulation of Cyclin D1 levels in both Jeko-1 and Z138C cells (Fig. 5a). sh-RNA-mediated knockdown of HDAC6 induces more phosphorylation of H2AX compared to NT-shRNA in Jeko-1 cells, in response to treatment with CB-508. Both Jeko-1 and Z138C cells show enhanced activation of caspase 3 in response to treatment with CB-5083 following HDAC6 knockdown (Fig. 5b).

Earlier studies have demonstrated that HDAC6-mediated deacetylation of HSP90 is essential for the conformational stability/chaperoning of key HSP90 client proteins including those involved in DNA repair, such as BRCA1 and ATR [15, 16, 34, 35]. We therefore hypothesized that combined inhibition of p97 and HDAC6 would severely impair HSP90-dependent chaperoning of DNA repair proteins in MCL cells [15, 34–36]. Consistent with this hypothesis, we observed that while treatment with ACY-1215 results in the partial depletion of HSP90 client proteins BRCA1 and CDK4 but not ATR, co-treatment with CB-5083 and ACY-1215 leads to their enhanced depletion (Fig. 5c). This is accompanied by increased cleavage of caspase 3 and marked downregulation of Cyclin D1.

Effect of co-treatment of CB-5083 and ACY-1215 in primary MCL cells

We next determined whether co-treatment with CB-5083 and ACY-1215 induced synergistic apoptosis in cultured MCL cells. We observed that the combination treatment shows synergistic interaction in primary MCL cells (Fig. 6a), with CI values for the combination treatments

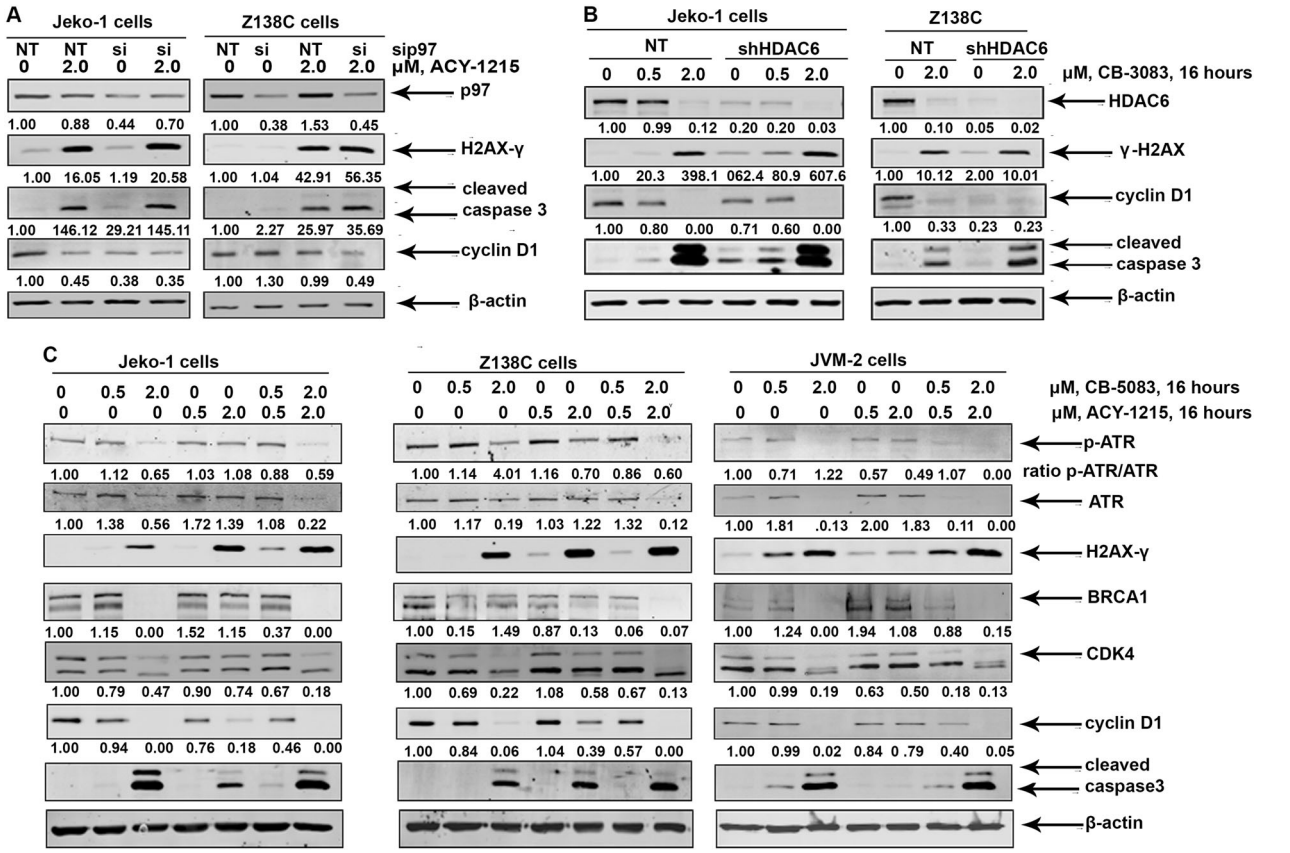

Fig. 5 Knockdown of p97 accentuates the accumulation of DSBs in response to ACY-1215 treatment. **a** Jeko-1 and Z138C cells were transfected with non-targeted (NT) RNA or p97 siRNA for 36 h and then treated with ACY-1215 for an additional 16 h. The cells were harvested and the expression of the indicated proteins was determined by western blot analysis. **b** HDAC6 was knocked down in Jeko-1 and Z138C cells and treated with CB-5083 for 16 h. The expression of H2AX-γ and indicated markers was determined by immunoblot analysis. **c** Jeko-1 and Z138C cells were exposed to CB-5083 and ACY-1215 or their combination for 16 h and the resultant cell lysates were utilized to perform immunoblot analysis

ranging from 0.3 to 0.8. Consistent with the observed induction of DNA damage in cultured MCL cells, co-treatment with CB-5083 and ACY-1215 induces the expression of H2AX-γ in primary MCL cells compared to treatment with single agent alone (Fig. 6b). Similar results were observed in primary MCL cells co-treated with ML-240 and ACY-1215 (Fig. 6c).

Co-treatment with CB-5083 and ACY-1215 impairs radiation-induced DNA repair mechanisms in MCL cells

To further explore the effect of both p97 and HDAC6 inhibition on the ability of MCL cells to resolve DSBs, we subjected MCL cells to 3 Gy ionizing radiation (IR) and determined the ability of MCL cells to repair damaged DNA. Exposure of MCL to IR resulted in the appearance of H2AX-γ foci at 1 h (Supplementary Figure S3), which resolved during recovery at 6 h in control cells (Fig. 7a). However, the combination of CB-5083 and ACY-1215 treatment resulted in sustained H2AX-γ foci at the end of 6 h of recovery (Fig. 7b). Furthermore, 53BP1 foci co-localized with H2AX-γ foci at 1 h (Supplementary Figure 3SA) but did not readily resolve at 6 h unlike the H2AX-γ foci, consistent with the delayed kinetics of resolution of 53BP1 foci compared to H2AX-γ foci [37].

Next, we determined the effect of CB-5083 and ACY-1215 treatments on signaling events upstream of loading of 53BP1 onto DSBs. 53BP1 is phosphorylated by ATM and ATR kinases and rapidly localizes to sites of DSBs following DNA damage and co-localizes with H2AX-γ foci in a p97-dependent manner [11, 37–39]. We observed that while treatment CB-5083 does not inhibit the phosphorylation of 53BP1, treatment with ACY-1215 reduces the levels of 53BP1 phosphorylation (Fig. 7c). We also observed that co-treatment with CB-5083 and ACY-1215 results in greater inhibition of 53BP1 phosphorylation in Z138C cells (and Supplementary Figure 3SB). The implications of these observation are discussed below.

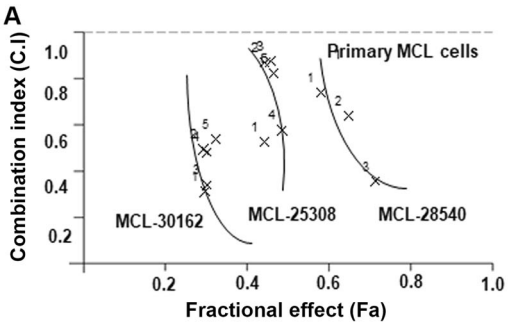

MCL-30162 (peripheral blood)

CB-5083 (μM)	ACY-1215 (μM)	Fa	CI
0.50	1.00	0.318	0.373
0.50	2.00	0.315	0.544
0.75	0.75	0.323	0.400
1.00	1.00	0.323	0.533
2.00	2.00	0.347	0.586

MCL-25308 (bone marrow)

CB-5083 (μM)	ACY-1215 (μM)	Fa	CI
0.75	1.00	0.553	0.552
0.75	2.00	0.553	0.862
1.00	2.00	0.567	0.868
1.50	1.00	0.596	0.597
1.50	1.50	0.576	0.821

MCL-28540 (lymph node)

CB-5083 (μM)	ACY-1215 (μM)	Fa	CI
1.50	1.50	0.646	0.845
2.00	0.50	0.722	0.747
2.00	1.00	0.796	0.466

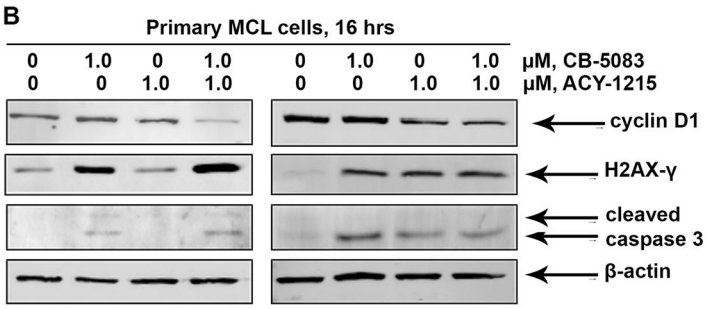

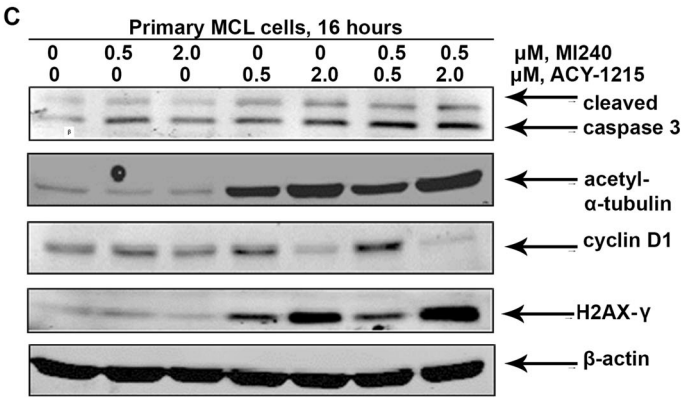

Fig. 6 Co-treatment with CB-5083 and ACY-1215 induces synergistic apoptosis in primary MCL cells. **a** Primary MCL cells were exposed to CB-5083 and ACY-125 for 24 h and percent apoptotic cells were determined. Fa and CI plot is presented. **b**, **c** Primary MCL cells were exposed to the indicated doses of p97 inhibitors and ACY-1215 for 16 h and the expression of Cyclin D1, H2AX-γ, cleaved-caspase 3, and actin were determined by immunoblot analysis

In vivo effect of CB-5083 treatment on MCL xenografts

Finally, we tested the activity of CB-5083 and ACY-1215 treatment on Z138C xenografts in NSG mice in vivo. Following injection of 2.5 million Z138C cells into the flanks of mice ($N = 6$ per group), we commenced treatment with CB-5083 and ACY-1215 for 2 weeks when the average tumor size reached 200 mm^3. Treatment with CB-5083 and ACY-1215 showed significant reduction in tumor volume by weeks 2 and 3 compared to CB-5083-treated mice (Fig. 8a). Kaplan–Meier survival analysis showed that mice receiving the combination of CB-5083 and ACY-1215 showed improved survival ($p = 0.04$) compared to CB-5083-treated mice (Fig. 8b). Consistent with the observed in vitro results, co-treatment with CB-5083 and ACY-1215 treatment also induced the accumulation of H2AX-γ in tumor cell lysates (Supplementary Figure 4SA), with little or no change in the expression of markers of ER stress (data not shown). Jeko-1 xenografts also showed reduced tumor volumes and improved survival in treatment groups compared to vehicle-treated mice (Supplementary figure 4SB and Fig. 8c).

Discussion

Targeting cellular protein quality control mechanisms has emerged as a promising strategy in MCL and multiple myeloma [8, 40–42]. Efforts to identify targets that work together with the ubiquitin–proteasome system and facilitate protein quality control led to the identification of CB-5083 as a highly specific p97 ATPase inhibitor with 60-fold weaker in vitro IC_{50} for DNA-dependent protein kinase (DNAPK) [25, 26]. Earlier studies have reported the synergistic activity of CB-5083 with proteasome inhibitors in pre-clinical models of multiple myeloma [43]. In this study, we report the anti-MCL activity of CB-5083 in

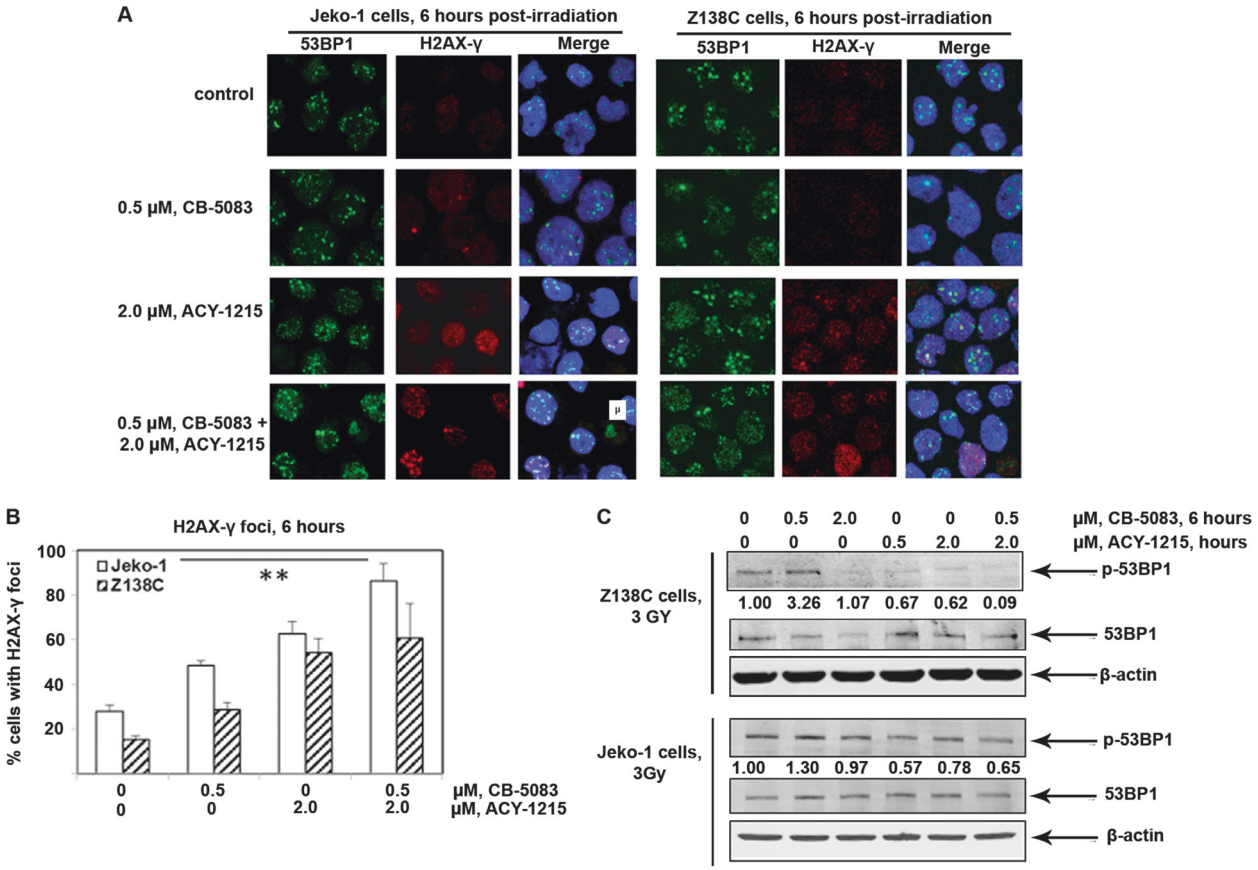

Fig. 7 Co-treatment with ACY-1215 and CB-5083 impairs the ability of MCL cells to repair DSBs. **a** Jeko-1 and Z138C cells were exposed 3 Gy IR and treated with CB-5083, ACY-1215 or the combination of the two agents and allowed to recover for at 37 °C for 6 h. The cells were then immunostained for 53BP1 and H2AX-γ. **b** The fraction of cells (from an average of 300 cells) with H2AX-γ foci at the end of 6 h were counted and plotted. Data are representative of three independent experiments. **c** Alternatively, MCL cells were exposed to indicated-doses of CB-5083 and ACY-1215 or their combination and irradiated. The resultant lysates were immunoblotted for p-53BP1, 53BP1, and β-actin

combination with ACY-1215 in MCL cells. Z138C cells show the least sensitivity to treatment with CB-5083, even though they respond to p97 inhibition by upregulating the levels of polyubiquitylated proteins and the CHOP. This suggests that factors other than those that compromise ERAD play a role in conferring sensitivity to p97 inhibition in MCL cells.

Unlike other reported p97 inhibitors, we observed that CB-5083 did not result in a significant increase in the accumulation of LC3B-II in Z138C and Jeko-1 cells (Fig. 4a). Additionally, treatment with CB-5083 or co-treatment with CB-5083 and ACY-1215 resulted in the degradation of p62 even in the presence of chloroquine. We therefore conclude that enhanced degradation of p62 could be attributed to incomplete inhibition of lysosomes in chloroquine and CB-5083-treated cells. The ubiquitin ligase Parkin-dependent ubiquitylation and degradation of p62 by the proteasomes in response to proteotoxic stress could also contribute to the observed p62 degradation [44, 45]. Further studies are required to elucidate the non-autophagolysosomal mechanisms that participate in the clearance of p62 in MCL cells treated with p97 and HDAC6 inhibitors.

Enhanced expression and stabilization of Cyclin D1 has been proposed to confer survival advantage to MCL cells [1, 46]. Consistent with earlier reports, our studies also suggest that downregulation of Cyclin D1 in MCL cells results in the enhanced DNA damage and susceptibility to other anti-cancer agents [47]. Furthermore, the down-regulation of CDK4 with both CB-5083 and ACY-1215 treatment, could also contribute to the anti-MCL activity of the combination [48]. The observed effect of ACY-1215 treatment on the depletion of Cyclin D1 could be an indirect effect of HSP90 inhibition on the activity of glycogen synthase kinase 3 beta, which phosphorylates and stabilizes Cyclin D1 [49]. Recent studies also suggest that the CDK-dependent phosphorylation of p97 promotes Cyclin D1 translocation from the ER and its nuclear localization [50]. This observation further supports our findings that loss of CDK4-function and/or activity following HDAC6

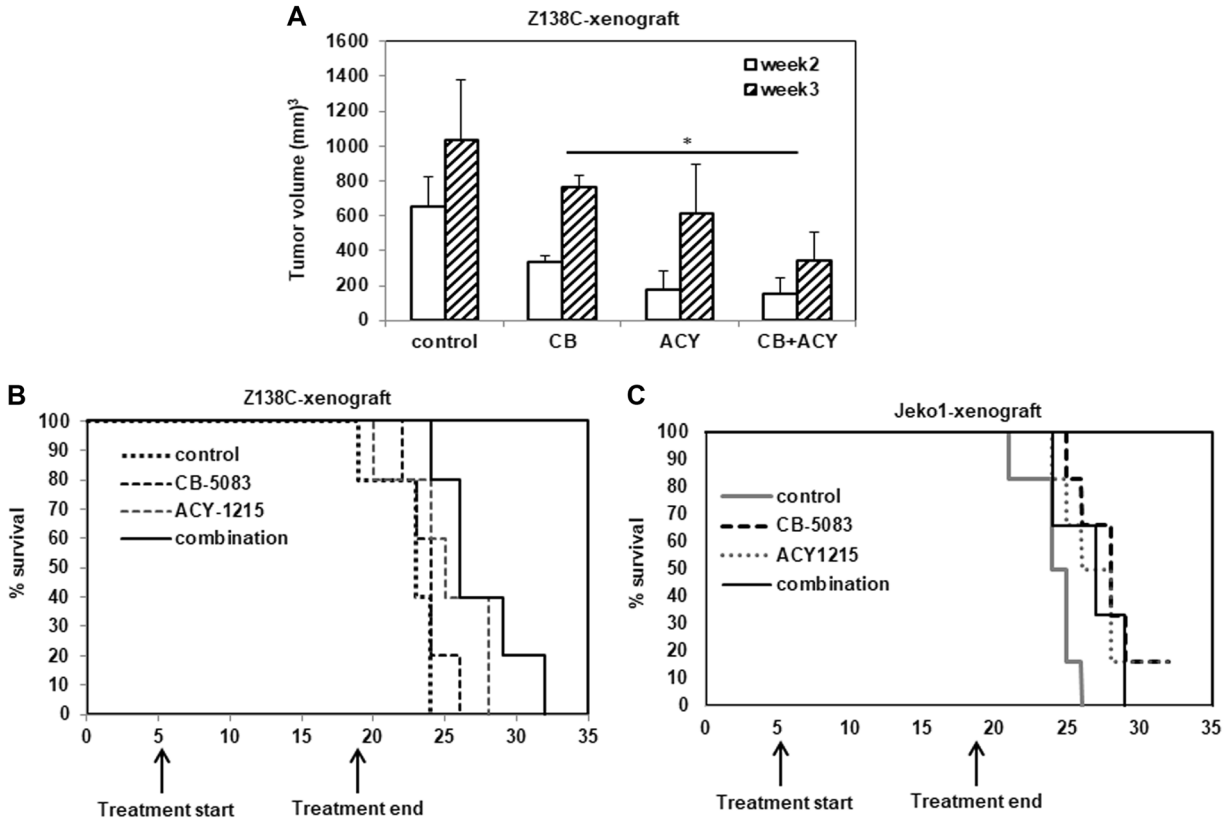

Fig. 8 Co-treatment with CB-5083 and ACY-1215 reduces tumor burden and improves survival in Z138C and Jeko-1 xenografts. **a** Average tumor volumes as measured at the end of week 2 and 3 after the injection of cells is presented. **b** Survival of mice in control and treated groups was determined by Kaplan–Meier plot analysis ($p = 0.04$ for CB-5083 versus combination treatment). **c** Survival analysis for Jeko-1 xenografts ($p = 0.05$ for control versus CB-5083 group and $p = -0.03$ for control versus combination group)

inhibition, in addition to p97 inhibition could culminate in Cyclin D1 degradation in MCL cells.

Another interesting finding described in this study pertains to the potentiation of DNA damaging effects of HDAC6 inhibitors [51]. Our studies reveal that co-treatment with CB-5083 and ACY-1215 treatment induces DNA damage and result in the downregulation of BRCA1 and total ATR proteins in MCL cells. The differential effect of ACY-1215 on depletion of BRCA1 in Z138C compared to Jeko-1 cells suggests that kinetics of degradation of individual HSP90 client proteins are governed by additional factors. Nevertheless, the significant decrease in the levels of BRCA1 in response to co-treatment with CB-5083 and ACY-1215 argues that both agents indeed affect BRCA1-dependent DNA repair [16], by HR, interstrand crosslinks and alternate NHEJ [52, 53]. Indeed, earlier studies have demonstrated that siRNA-mediated depletion of p97 results in significant decrease in the percentage of HR without affecting NHEJ pathway in osteosarcoma cell lines [13]. Additionally, p53BP1 phosphorylation is most affected in Z138C cells which are *ATM*-deleted as compared to other cell lines which show *ATM* gain (Jeko-1, Rec1) or possess wildtype *ATM* (JVM-2) (Fig. 7c and Supplementary Figure 3B). These results are consistent irrespective of the *p53* status in the cell lines tested as Z138C and JVM-2 cells possess wild type p53 and Jeko-1 and Rec1 cells harbor p53 mutations. This is consistent with the fact that *ATM* is upstream to *p53* activation [3].

Collectively, our studies suggest that p97 inhibitors induce synergistic cell death in MCL cells in combination with HDAC6 inhibitors by inducing ER stress, depleting CDK4, CyclinD1, BRCA1, and ATR. These observations suggest that dysregulation of proteostasis and impaired DNA repair mechanisms contribute to the synergistic apoptotic activity of the p97 and HDAC6 inhibitors. These studies create a strong rationale to test the safety and efficacy of the combination of p97 inhibitors and ACY-1215 in human MCL.

Acknowledgements The authors wish to acknowledge the Biorepository Core Facility of the University of Kansas Cancer Center for providing primary MCL and normal blood samples. RR is a recipient of the American Cancer Society-Institutional Research Grant (ACS-IRG-16-194-07). RAJ is a recipient of P30 CA168524 from NCI.

Compliance with ethical standards

Conflict of interest The authors declare that they have no conflict of interest.

Publisher's note: Springer Nature remains neutral with regard to jurisdictional claims in published maps and institutional affiliations.

References

1. Vogt N, Dai B, Erdmann T, Berdel WE, Lenz G. The molecular pathogenesis of mantle cell lymphoma. Leuk Lymphoma. 2017;58:1530–7.
2. Ahmed M, Zhang L, Nomie K, Lam L, Wang M. Gene mutations and actionable genetic lesions in mantle cell lymphoma. Oncotarget. 2016;7:58638–48.
3. Bea S, Valdes-Mas R, Navarro A, Salaverria I, Martin-Garcia D, Jares P, et al. Landscape of somatic mutations and clonal evolution in mantle cell lymphoma. Proc Natl Acad Sci USA. 2013;110:18250–5.
4. Rao R, Nalluri S, Fiskus W, Savoie A, Buckley KM, Ha K, et al. Role of CAAT/enhancer binding protein homologous protein in panobinostat-mediated potentiation of bortezomib-induced lethal endoplasmic reticulum stress in mantle cell lymphoma cells. Clin Cancer Res. 2010;16:4742–54.
5. Vekaria PH, Home T, Weir S, Schoenen FJ, Rao R. Targeting p97 to disrupt protein homeostasis in cancer. Front Oncol. 2016;6:181.
6. Meyer H, Weihl CC. The VCP/p97 system at a glance: connecting cellular function to disease pathogenesis. J Cell Sci. 2014;127:3877–83.
7. Rabinovich E, Kerem A, Frohlich KU, Diamant N, Bar-Nun S. AAA-ATPase p97/Cdc48p, a cytosolic chaperone required for endoplasmic reticulum-associated protein degradation. Mol Cell Biol. 2002;22:626–34.
8. Anderson DJ, Le Moigne R, Djakovic S, Kumar B, Rice J, Wong S, et al. Targeting the AAA ATPase p97 as an approach to treat cancer through disruption of protein homeostasis. Cancer Cell. 2015;28:653–65.
9. Bastola P, Neums L, Schoenen FJ, Chien J. VCP inhibitors induce endoplasmic reticulum stress, cause cell cycle arrest, trigger caspase-mediated cell death and synergistically kill ovarian cancer cells in combination with Salubrinal. Mol Oncol. 2016;10:1559–74.
10. Jowsey P, Morrice NA, Hastie CJ, McLauchlan H, Toth R, Rouse J. Characterisation of the sites of DNA damage-induced 53BP1 phosphorylation catalysed by ATM and ATR. DNA Repair. 2007;6:1536–44.
11. Acs K, Luijsterburg MS, Ackermann L, Salomons FA, Hoppe T, Dantuma NP. The AAA-ATPase VCP/p97 promotes 53BP1 recruitment by removing L3MBTL1 from DNA double-strand breaks. Nat Struct Mol Biol. 2011;18:1345–50.
12. Torrecilla I, Oehler J, Ramadan K. The role of ubiquitin-dependent segregase p97 (VCP or Cdc48) in chromatin dynamics after DNA double strand breaks. Philos Trans R Soc Lond B 2017;372 (1731):20160282.
13. van den Boom J, Wolf M, Weimann L, Schulze N, Li F, Kaschani F, et al. VCP/p97 extracts sterically trapped Ku70/80 rings from DNA in double-strand break repair. Mol Cell. 2016;64:189–98.
14. Boyault C, Zhang Y, Fritah S, Caron C, Gilquin B, Kwon SH, et al. HDAC6 controls major cell response pathways to cytotoxic accumulation of protein aggregates. Genes Dev. 2007;21:2172–81.
15. Bali P, Pranpat M, Bradner J, Balasis M, Fiskus W, Guo F, et al. Inhibition of histone deacetylase 6 acetylates and disrupts the chaperone function of heat shock protein 90: a novel basis for antileukemia activity of histone deacetylase inhibitors. J Biol Chem. 2005;280:26729–34.
16. Stecklein SR, Kumaraswamy E, Behbod F, Wang W, Chaguturu V, Harlan-Williams LM, et al. BRCA1 and HSP90 cooperate in homologous and non-homologous DNA double-strand-break repair and G2/M checkpoint activation. Proc Natl Acad Sci USA. 2012;109:13650–5.
17. Rao R, Fiskus W, Yang Y, Lee P, Joshi R, Fernandez P, et al. HDAC6 inhibition enhances 17-AAG-mediated abrogation of hsp90 chaperone function in human leukemia cells. Blood. 2008;112:1886–93.
18. Taipale M, Jarosz DF, Lindquist S. HSP90 at the hub of protein homeostasis: emerging mechanistic insights. Nat Rev Mol Cell Biol. 2010;11:515–28.
19. Lee JY, Koga H, Kawaguchi Y, Tang W, Wong E, Gao YS, et al. HDAC6 controls autophagosome maturation essential for ubiquitin-selective quality-control autophagy. EMBO J. 2010;29:969–80.
20. Kawaguchi Y, Kovacs JJ, McLaurin A, Vance JM, Ito A, Yao TP. The deacetylase HDAC6 regulates aggresome formation and cell viability in response to misfolded protein stress. Cell . 2003;115:727–38.
21. Santo L, Hideshima T, Kung AL, Tseng JC, Tamang D, Yang M, et al. Preclinical activity, pharmacodynamic, and pharmacokinetic properties of a selective HDAC6 inhibitor, ACY-1215, in combination with bortezomib in multiple myeloma. Blood. 2012;119:2579–89.
22. Fiskus W, Saba N, Shen M, Ghias M, Liu J, et al. Auranofin induces lethal oxidative and endoplasmic reticulum stress and exerts potent preclinical activity against chronic lymphocytic leukemia. Cancer Res. 2014;2014:2520–32.
23. Shen D, Coleman J, Chan E, Nicholson TP, Dai L, Sheppard PW, et al. Novel cell- and tissue-based assays for detecting misfolded and aggregated protein accumulation within aggresomes and inclusion bodies. Cell Biochem Biophys. 2011;60:173–85.
24. Chou TF, Li K, Frankowski KJ, Schoenen FJ, Deshaies RJ. Structure–activity relationship study reveals ML240 and ML241 as potent and selective inhibitors of p97 ATPase. ChemMedChem. 2013;8:297–312.
25. Chou TF, Brown SJ, Minond D, Nordin BE, Li K, Jones AC, et al. Reversible inhibitor of p97, DBeQ, impairs both ubiquitin-dependent and autophagic protein clearance pathways. Proc Natl Acad Sci USA. 2011;108:4834–9.
26. Zhou HJ, Wang J, Yao B, Wong S, Djakovic S, Kumar B. et al. Discovery of a first-in-class, potent, selective, and orally bioavailable inhibitor of the p97 AAA ATPase (CB-5083). J Med Chem. 2015;58:9480–97.
27. Magnaghi P, D'Alessio R, Valsasina B, Avanzi N, Rizzi S, Asa D, et al. Covalent and allosteric inhibitors of the ATPase VCP/p97 induce cancer cell death. Nat Chem Biol. 2013;9:548–56.
28. Clarke HJ, Chambers JE, Liniker E, Marciniak SJ. Endoplasmic reticulum stress in malignancy. Cancer Cell. 2014;25:563–73.
29. Hubbert C, Guardiola A, Shao R, Kawaguchi Y, Ito A, Nixon A, et al. HDAC6 is a microtubule-associated deacetylase. Nature. 2002;417:455–8.
30. Ogata M, Hino S, Saito A, Morikawa K, Kondo S, Kanemoto S. et al.Autophagy is activated for cell survival after endoplasmic reticulum stressMol Cell Biol.2006;26:9220–31.
31. Feng Y, He D, Yao Z, Klionsky DJ. The machinery of macroautophagy. Cell Res.2014;24:24–41.
32. Fornace AJ Jr., Nebert DW, Hollander MC, Luethy JD, Papathanasiou M, Fargnoli J, et al. Mammalian genes coordinately regulated by growth arrest signals and DNA-damaging agents. Mol Cell Biol. 1989;9:4196–203.

33. Oyadomari S, Mori M. Roles of CHOP/GADD153 in endoplasmic reticulum stress. Cell Death Differ. 2004;11:381–9.
34. Ha K, Fiskus W, Rao R, Balusu R, Venkannagari S, Nalabothula NR, et al. Hsp90 inhibitor-mediated disruption of chaperone association of ATR with hsp90 sensitizes cancer cells to DNA damage. Mol Cancer Ther. 2011;10:1194–206.
35. Kovacs JJ, Murphy PJ, Gaillard S, Zhao X, Wu JT, Nicchitta CV, et al. HDAC6 regulates Hsp90 acetylation and chaperone-dependent activation of glucocorticoid receptor. Mol Cell. 2005;18:601–7.
36. Pennisi R, Ascenzi P, di Masi A. Hsp90: a new player in DNA repair? Biomolecules. 2015;5:2589–618.
37. Harding SM, Coackley C, Bristow RG. ATM-dependent phosphorylation of 53BP1 in response to genomic stress in oxic and hypoxic cells. Radiother Oncol. 2011;99:307–12.
38. Anderson L, Henderson C, Adachi Y. Phosphorylation and rapid relocalization of 53BP1 to nuclear foci upon DNA damage. Mol Cell Biol. 2001;21:1719–29.
39. Her J, Ray C, Altshuler J, Zhang H, Bunting SF. 53BP1 mediates ATR-Chk1 signaling and protects replication forks under conditions of replication stress. Mol Cell Biol. 2018;e00472–17.
40. Fisher RI, Bernstein SH, Kahl BS, Djulbegovic B, Robertson MJ, de Vos S, et al. Multicenter phase II study of bortezomib in patients with relapsed or refractory mantle cell lymphoma. J Clin Oncol. 2006;24:4867–74.
41. Holkova B, Grant S. Proteasome inhibitors in mantle cell lymphoma. Best Pract Res Clin Haematol. 2012;25:133–41.
42. Manasanch EE, Orlowski RZ. Proteasome inhibitors in cancer therapy. Nat Rev Clin Oncol. 2017;14:417–33.
43. Le Moigne R, Aftab BT, Djakovic S, Dhimolea E, Valle E, Murnane M, et al. The p97 inhibitor CB-5083 is a unique disrupter of protein homeostasis in models of multiple myeloma. Mol Cancer Ther. 2017;16:2375–86.
44. Song P, Li S, Wu H, Gao R, Rao G, Wang D, et al. Parkin promotes proteasomal degradation of p62: implication of selective vulnerability of neuronal cells in the pathogenesis of Parkinson's disease. Protein Cell. 2016;7:114–29.
45. Seibenhener ML, Babu JR, Geetha T, Wong HC, Krishna NR, Wooten MW. Sequestosome 1/p62 is a polyubiquitin chain binding protein involved in ubiquitin proteasome degradation. Mol Cell Biol. 2004;24:8055–68.
46. Deshpande A, Pastore A, Deshpande AJ, Zimmermann Y, Hutter G, Weinkauf M, et al. 3'UTR mediated regulation of the cyclin D1 proto-oncogene. Cell Cycle. 2009;8:3592–600.
47. Mohanty S, Mohanty A, Sandoval N, Tran T, Bedell V, Wu J, et al. Cyclin D1 depletion induces DNA damage in mantle cell lymphoma lines. Leuk Lymphoma. 2017;58:676–88.
48. Marzec M, Kasprzycka M, Lai R, Gladden AB, Wlodarski P, Tomczak E, et al. Mantle cell lymphoma cells express predominantly cyclin D1a isoform and are highly sensitive to selective inhibition of CDK4 kinase activity. Blood. 2006;108:1744–50.
49. Banz VM, Medova M, Keogh A, Furer C, Zimmer Y, Candinas D, et al. Hsp90 transcriptionally and post-translationally regulates the expression of NDRG1 and maintains the stability of its modifying kinase GSK3beta. Biochim Biophys Acta. 2009;1793:1597–603.
50. Parisi E, Yahya G, Flores A, Aldea M. Cdc48/p97 segregase is modulated by cyclin-dependent kinase to determine cyclin fate during G1 progression. EMBO J 2018;37:e98724.
51. Namdar M, Perez G, Ngo L, Marks PA. Selective inhibition of histone deacetylase 6 (HDAC6) induces DNA damage and sensitizes transformed cells to anticancer agents. Proc Natl Acad Sci USA. 2010;107:20003–8.
52. Saha J, Davis AJ. Unsolved mystery: the role of BRCA1 in DNA end-joining. J Radiat Res. 2016;57(Suppl. 1):i18–i24.
53. Bunting SF, Callen E, Kozak ML, Kim JM, Wong N, Lopez-Contreras AJ, et al. BRCA1 functions independently of homologous recombination in DNA interstrand crosslink repair. Mol Cell. 2012;46:125–35.